Proceedings of the Canadian Society for Mechanical Engineering International Congress 2022
CSME Congress 2022
June 5-8, 2022, Edmonton, AB, Canada

Combination of AC electrothermal and Dielectrophoresis realized by 3D Electrodes to Concentrate Particles

Jino Fathy[1*], Ziying Wang[1], Yongjun Lai[1]
[1]Department of Mechanical and Materials Engineering, Queen`s University, Kingston, Canada
*17jf14@queensu.ca

Abstract**—** In this paper, a particle microconcentrator is designed and simulated that works by combining the AC electrothermal (ACET) and Dielectrophoresis (DEP) forces. The microconcentrator consists of a PMMA channel with copper electrodes on the walls and bottom of the channel. On each side of the channel, two coplanar asymmetric electrodes are fixed. 10Vp voltage with a frequency of 500kHz is applied to the bigger electrodes and the smaller electrodes are grounded. The bottom electrode is a floating potential and not connected to any electric source. COMSOL Multiphysics v6 was used to simulate the electric field, heat transfer, and ACET induced vortices in the fluid. Then, the ACET and DEP forces were applied to the modeled polystyrene particles with a diameter of 6µm. Both forces affect the particles focusing, while the effect of ACET is stronger.

Keywords-component; AC electrothermal; Dielectrophoresis; Microconcentrator; Simulation

I. INTRODUCTION

Microconcentrators are important components in microfluidic systems to increase the concentration of particles. They are especially beneficial in biosensing applications to address the need for real-time detection of biological particles in low concentrations. By having a higher concentration of bio-analytes compared to the initial dilute sample, the particles have a better chance of being detected in a shorter time.

AC electrokinetic (ACEK) is a well-known technique used in microfluidics to move fluid and/or particles by applying an electric field. AC electrothermal (ACET) and dielectrophoresis (DEP) are two of the ACEK techniques which are used in this work. By setting parameters such as the medium conductivity and the frequency of the electric field either one or both forces might be available or dominant. DEP is a short-range force and decays exponentially by getting further from the electrodes. On the other hand, the ACET vortices may trap the particles. Combining these two effects improves the particle manipulation techniques and bring advantages to some applications like biosensing and cell manipulation [1]–[4].

Both ACET and DEP have a wide range of applications in microfluidics. Some of the ACET applications are fluid pumping and mixing [5]–[7]. DEP is a versatile technique with some applications such as particle separation [8], [9]. In addition, they are both useful in particle concentration [10], [11].

Electrode structures are used inside the channels to create the electric field non-uniformity required to apply ACET and/or DEP forces on the fluid and the particles suspended in it. Changing the shape and size of the electrodes alternates the electric field distribution which in turn changes the performance of the microconcentrator. Most of the designs have planar electrodes, mainly at the bottom of the channel to apply DEP, ACET, or a combination of them [12]–[14]. However, the benefits of the 3D electrodes motivate the researchers to implement them in their designs. Some of the 3D electrode designs are presented in [8], [11], [15], [16].

In this work, a designed particle microconcentrator is presented that works by combining the ACET and DEP effects. Electrodes are placed on the walls of the channel and one electrode, not connected to electric potential, is placed at the bottom of the channel. The design is modeled in COMSOL Multiphysics v6 and the forces inside the channel are simulated and applied to the modeled polystyrene (PS) particles. The forces push the particles to the channel center.

II. THEORY

A. DEP

DEP is a force that is applied to polarizable particles in a non-uniform electric field. It can move the particles toward the higher electric field areas (positive DEP, pDEP) or against it (negative DEP, nDEP). The time-averaged formula of DEP is [17]:

$$\langle F_{DEP} \rangle = 2\pi\varepsilon_0\varepsilon_m r^3 Re\left[\tilde{f}_{CM}\right]\nabla|E_{rms}|^2 \tag{1}$$

Where, ε_0 and ε_m are the vacuum and the suspending medium permittivity, respectively, r is the particle radius, and E_{rms} is the root-mean-squared electric field strength. $\mathrm{Re}[\tilde{f}_{CM}]$ corresponds to the real part of the Clausius–Mossotti (CM) factor, which its sign indicates if the force is pDEP or nDEP.

B. ACET

AC electric field creates local heating in the fluid which results in permittivity and conductivity gradients. This, in turn, yields a body force on the fluid which is ACET force and leads to the creation of vortices around the electrodes. The temperature gradient can be obtained by solving the energy balance equation [17], [18]:

$$k\nabla^2 T + \langle \sigma |E|^2 \rangle = 0 \quad (2)$$

Where, k and σ are the thermal and electrical conductivity of the fluid, respectively. T is temperature and E is the electric field.

The time-averaged ACET force exerted on a fluid can be written as [19]:

$$\langle F_{et} \rangle = -\frac{1}{2}\varepsilon\left[0.024\nabla T.E\frac{E}{1+(\omega\tau)^2} - 0.002.|E|^2.\nabla T\right] \quad (3)$$

Where, ω and τ are the angular frequency and the charge relaxation time, respectively.

III. Design and Simulation

The microconcentrator consists of two pairs of coplanar asymmetric electrodes on the sidewalls and one floating electrode on the bottom of the channel. Fig. 1. depicts the modeled microconcentrator. The electrodes are located on the walls to make 3D AC electrokinetic effects. The channel has a rectangular cross section (1mm×1.5mm). The bigger and smaller electrodes on each side are 500 µm and 250 µm wide, respectively. The modelled channel in the simulation has a length of 3mm.

The suggested prototyping process for this microconcentrator is to use 3 PMMA (Polymethy methacrylate) plates and glue them together by thin layers of PDMS (Polydimethylsiloxane). The top and middle PMMA plates are laser cut to create the channel and the inlet and outlet holes. Also, copper tapes (80 µm thick, adhesive on one side) are cut and used as the electrodes.

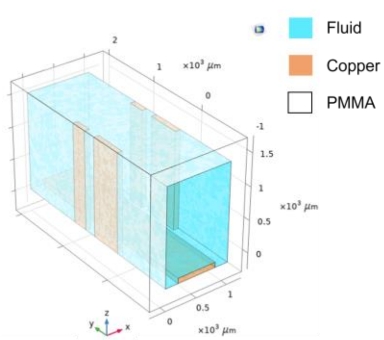

Figure 1. Schematic of the 3D model used to simulate the particle concentration.

In this paper, we only discuss the 3D FEM simulation of the particle concentrator conducted by COMSOL Multiphysics v6. The electric currents, heat transfer, laminar flow, and particle tracing physics modules were utilized. The model was meshed in fine size. The boundary conditions and studies for each module are as below:

Electric field: The “electric currents” module was used to simulate the electric field. 10Vp was applied to the bigger electrodes and the smaller ones were grounded. The electrode on the bottom of the channel was considered as floating potential, meaning it is an unconnected conductive electrode. All other surfaces were considered electrically insulated. The electric field was solved in the frequency domain with a frequency of 500kHz. The fluid has an high electrical conductivity of 0.224 S/m.

Joule heating: The “heat transfer in solids and fluids” module was used to simulate the thermal rise and solved with a stationary solution. The outer boundaries had room temperature (COMSOL default is 293.15 K). The PMMA and the copper electrodes were considered as two different solids with their characteristic material properties. The thermal conductivity for PMMA and copper are 0.19 and 401 [W/m*K], respectively. These values are from the default materials from the COMSOL material library. The material properties of the fluid such as its viscosity were temperature dependent. The inlet and outlet had an initial temperature of 293.15K. In addition, an “electromagnetic heating (emh)” sub-node was added to the “Multiphysics” node to account for the joule heating.

Fluidic: The “laminar flow” module was used for an incompressible flow. The ACET force was applied to the fluid as a body force by implementing Eq. 3 in accordance with the 3 axes. Navier-stokes equation was solved with a stationary study. The inlet had a velocity of 20um/s. This low velocity was considered to better see the effect of ACET and DEP on the particles. The outlet had zero pressure. The walls had no-slip boundary condition.

Particle tracing: The “particle tracing for fluid flow” module was used. Polystyrene (PS) particles with a 6 µm diameter and a density of 1050 kg/m^3 were modeled. The walls were simulated to bounce the particles back whenever they hit them, except for the outlet which was simulated to freeze the particles. The particles were released from specific locations inside the channel. Drag force and gravity were applied to the particles. In the DEP simulation, the DEP force is also applied to the particles. In the ACET simulation, the drag force node moves the particles to the channel center by the ACET vortices.

IV. Results and Discussion

Fig. 2 illustrates the electric field strength and temperature inside the channel from a top view. The higher electric field occurs in the gap between the two coplanar electrodes. The temperature is the highest on the electrode surfaces and around them.

Fig.3 shows the vortices in the fluid created by ACET in a longitude cross-section of the channel (top view). The surface plot shows the fluid velocity in the y-direction (length of the

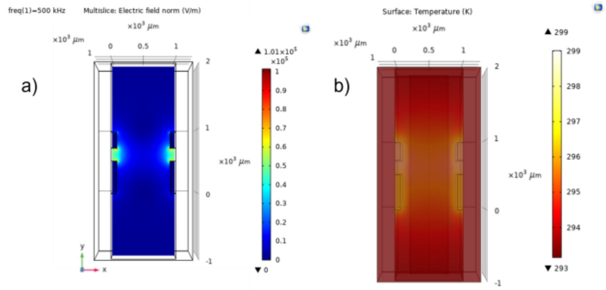

Figure 2. a) the electric field distribution inside the microchannel. B) The temperature inside of the microchannel as a result of applying the electric field.

channel), and the magnitude-controlled streamline shows the fluid velocity field.

Fig. 4 demonstrates a top view (x-y plane) and side view (x-z plane) of the particles focused to the center of the channel affected by the ACET vortices. Figures 4 a and c show the initial location of the particles and Figures 4 b and d depict their final location. The lines show the path of the particles. Their color represents the particles' velocity magnitude.

Fig. 5 shows the effect of DEP on the particle's movement. Particles have the same initial positions. As the conductivity of the medium is high, the DEP effect is not strong. However, as it has been discussed in [1] by changing the medium conductivity and frequency of the electric field, DEP can be more effective. Also, the big size of the electrodes compared with the particles` size causes the DEP effect to be weak as discussed in [8]. By optimizing the design to have smaller electrodes, DEP can be higher.

V. CONCLUSION

The design and simulation of a particle microconcentrator was presented. The microconcentrator works based on a combination of the ACET and DEP effects. COMSOL simulations were presented to show the electric field, the temperature inside the channel and the ACET inducted vortices inside the fluid. Polystyrene particles with a 6µm diameter were modeled and the effect of ACET and DEP forces on their focusing were studied. Both forces help the particles to move to the center of the channel. ACET is the stronger force due to very high conductivity of the medium and big size of the electrodes compared with the particles. For the future studies, various effective parameters can be investigated such as the frequency of the electric field, the conductivity of the medium, the size of the electrodes and the gap between the coplanar electrodes. Also, the effect of having multiple sets of the electrodes might be studied.

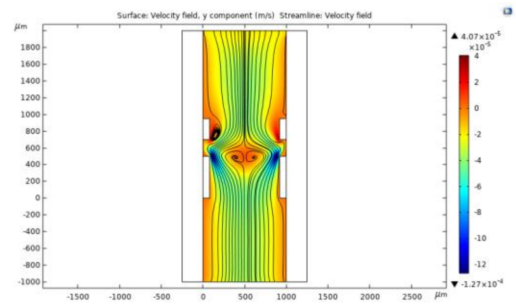

Figure 3. ACET vortices in the fluid. The surface shows the magnitude of the y component of the fluid velocity. The streamline depicts the velocity field.

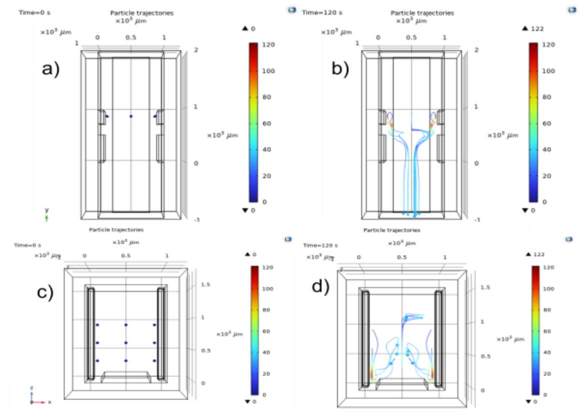

Figure 4. Focusing of the PS particles affected by ACET force. a) The particles' initial location (top view), b) The particles final location (top view), c) The particles' initial location (side view), d) The particles final location (side view).

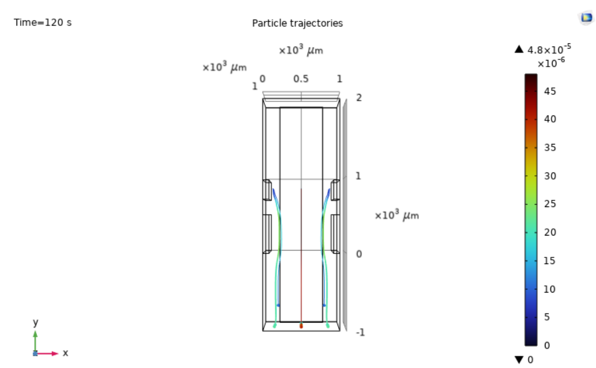

Figure 5. Cross-section view of the channel showing the movement of the particles affected by DEP force.

REFERENCES

[1] H. Sun, Y. Ren, Y. Tao, W. Liu, T. Jiang, and H. Jiang, "Combined alternating current electrothermal and dielectrophoresis-induced tunable patterning to actuate on-chip microreactions and switching at a floating electrode," *Sensors Actuators, B Chem.*, Feb. 2019, doi: 10.1016/j.snb.2019.127397.

[2] J. Meng *et al.*, "A single-step DNAzyme sensor for ultra-sensitive and rapid detection of Pb2+ ions," *Electrochim. Acta*, vol. 368, p. 137551, Feb. 2021,

doi: 10.1016/J.ELECTACTA.2020.137551.

[3] S. L. Tsai, Y. Chiang, M. H. Wang, M. K. Chen, and L. S. Jang, “Battery-powered portable instrument system for single-cell trapping, impedance measurements, and modeling analyses,” *Electrophoresis*, vol. 35, no. 16, pp. 2392–2400, Aug. 2014, doi: 10.1002/ELPS.201300591.

[4] H. Sun *et al.*, “Continuous Particle Trapping, Switching, and Sorting Utilizing a Combination of Dielectrophoresis and Alternating Current Electrothermal Flow,” *Anal. Chem.*, vol. 91, no. 9, pp. 5729–5738, May 2019, doi: 10.1021/ACS.ANALCHEM.8B05861/SUPPL_FILE/AC8B05861_SI_006.AVI.

[5] R. H. Vafaie, H. B. Ghavifekr, H. Van Lintel, J. Brugger, and P. Renaud, “Bi-directional ACET micropump for on-chip biological applications,” *Electrophoresis*, vol. 37, no. 5–6, pp. 719–726, 2016, doi: 10.1002/elps.201500404.

[6] R. H. Vafaie and H. B. Ghavifekr, “Configurable ACET micro-manipulator for high conductive mediums by using a novel electrode engineering,” *Microsyst. Technol.*, vol. 23, no. 5, pp. 1393–1403, 2017, doi: 10.1007/s00542-015-2806-y.

[7] J. Meng, S. Li, J. Li, C. Yu, C. Wei, and S. Dai, “AC electrothermal mixing for high conductive biofluids by arc-electrodes,” *J. Micromechanics Microengineering*, vol. 28, no. 6, p. 065004, Mar. 2018, doi: 10.1088/1361-6439/AAB39B.

[8] J. Fathy, A. Pourmand, and H. B. Ghavifekr, “Design and simulation of a MEMS based cell separator utilizing 3D travelling-wave dielectrophoresis,” *Microsyst. Technol.*, vol. 23, no. 5, pp. 1351–1360, May 2017, doi: 10.1007/s00542-015-2757-3.

[9] J. Fathy, A. Pourmand, and H. Badri Ghavifekr, “Utilizing electric field to separate cells with travelling-wave dielectrophoresis force in a droplet,” *2017 25th Iran. Conf. Electr. Eng. ICEE 2017*, no. lCEE20 17, pp. 435–439, 2017, doi: 10.1109/IranianCEE.2017.7985489.

[10] H. Sun, Y. Ren, Y. Tao, T. Jiang, and H. Jiang, “Flexible online in-droplet cell/synthetic particle concentration utilizing alternating current electrothermal-flow field-effect transistor,” *Lab Chip*, vol. 21, no. 10, pp. 1987–1997, May 2021, doi: 10.1039/D0LC01328E.

[11] J. Fathy and Y. Lai, “Utilizing a coil to realize 3D electrodes for dielectrophoresis-based particle concentration,” *J. Micromechanics Microengineering*, vol. 30, no. 3, 2020, doi: 10.1088/1361-6439/ab6c71.

[12] R. S. Thomas, H. Morgan, and N. G. Green, “Negative DEP traps for single cell immobilisation †,” doi: 10.1039/b819267g.

[13] R. Zhang, C. Dalton, and G. A. Jullien, “Two-phase AC electrothermal fluidic pumping in a coplanar asymmetric electrode array,” *Microfluid. Nanofluidics*, vol. 10, no. 3, pp. 521–529, Mar. 2011, doi: 10.1007/s10404-010-0686-0.

[14] L. S. Jang, P. H. Huang, and K. C. Lan, “Single-cell trapping utilizing negative dielectrophoretic quadrupole and microwell electrodes,” *Biosens. Bioelectron.*, vol. 24, no. 12, pp. 3637–3644, Aug. 2009, doi: 10.1016/J.BIOS.2009.05.027.

[15] A. Salari and C. Dalton, “Fast biofluid transport of high conductive liquids using AC electrothermal phenomenon , a study on substrate characteristics,” *Comsol*, 2014.

[16] A. Salari, M. Navi, and C. Dalton, “AC electrothermal micropump for biofluidic applications using numerous microelectrode pairs,” *2014 IEEE Conf. Electr. Insul. Dielectr. Phenomena, CEIDP 2014*, pp. 1–4, 2014, doi: 10.1109/CEIDP.2014.6995870.

[17] H. Morgan and N. G. Green, *AC Electrokinetics: colloids and nanoparticles*, no. C. Research Studies Press Ltd and Institute of Physics PUBLISHING, 2003.

[18] A. Salari and M. Thompson, “Recent advances in AC electrokinetic sample enrichment techniques for biosensor development,” *Sensors Actuators B Chem.*, vol. 255, pp. 3601–3615, Feb. 2018, doi: 10.1016/J.SNB.2017.09.069.

[19] A. Salari and C. Dalton, “A novel AC electrothermal micropump for biofluid transport using circular interdigitated microelectrode array,” *Microfluid. BioMEMS, Med. Microsystems XIII*, vol. 9320, no. March 2015, p. 932016, 2015, doi: 10.1117/12.2077794.